APPENDIX G
P-21-013 BUFFER CAR POST TEST ANALYSIS REPORT

BUFFER CAR
POST TEST ANALYSIS REPORT

Prepared for
United States Department of Energy

Report P-21-013

Revised June 23, 2021

PROPRIETARY REPORT

TTCI®
TRANSPORTATION
TECHNOLOGY CENTER, INC.

BUFFER CAR
POST TEST ANALYSIS REPORT

Prepared for
United States Department of Energy

Report P-21-013

Russell Walker
Matt DeGeorge
MaryClara Jones
Richard Joy
Nicholas Hinsch (Kasgro Rail)

Transportation Technology Center, Inc.
A subsidiary of the Association of American Railroads
Pueblo, Colorado USA

April 5, 2021
Revised June 23, 2021

Disclaimer: This report was prepared for The United States Department of Energy (DOE) by Transportation Technology Center, Inc. (TTCI), a subsidiary of the Association of American Railroads, Pueblo, Colorado. It is based on investigations and tests conducted by TTCI with the direct participation of DOE to criteria approved by them. The contents of this report imply no endorsements whatsoever by TTCI of products, services or procedures, nor are they intended to suggest the applicability of the test results under circumstances other than those described in this report. The results and findings contained in this report are the sole property of DOE. They may not be released by anyone to any party other than DOE without the written permission of DOE. TTCI is not a source of information with respect to these tests, nor is it a source of copies of this report. TTCI makes no representations or warranties, either expressed or implied, with respect to this report or its contents. TTCI assumes no liability to anyone for special, collateral, exemplary, indirect, incidental, consequential, or any other kind of damages resulting from the use or application of this report or its contents.

EXECUTIVE SUMMARY

The United States Department of Energy (DOE) contracted with Transportation Technology Center, Inc. (TTCI) to perform certification testing on its buffer railcar developed as part of DOE's Atlas Railcar Design Project. The intent of the project is to meet the needs for future large-scale transport of high-level radioactive material (HLRM) as defined in Association of American Railroads' (AAR) *Manual of Standards and Recommended Practices,* Standard S-2043, which includes spent nuclear fuel and high-level waste.

The buffer car met all S-2043 single-car structural and dynamic test requirements.

Finite element analysis (FEA) simulations and structural test strain measurements showed that stresses were less than 75 percent of the allowable stress, eliminating the requirement for FEA to be refined per Paragraph 8.1 of Standard S-2043. The largest difference between measured and predicted stress was 5.7 ksi.

The revised model did not meet the criterion for peak-to-peak carbody lateral acceleration for the 39-foot wavelength inputs (1.38g, limit = 1.3g) or the 44.5-foot wavelength inputs (1.31g, limit = 1.3g) in yaw and sway simulations. In contrast, the buffer car met test requirements for yaw and sway indicating that the model is conservative. The yaw and sway test is only performed with 39-foot wavelength inputs.

The revised modeling predictions did not meet S-2043 criteria for truck side lateral/vertical (L/V) ratio (0.52, limit = 0.5) in the curving with various lubrication conditions regime. This exception occurred for counterclockwise runs with Case 2 lubrication and the worn wheel profile at 12 and 24 mph. The Case 2 lubrication condition is a 0.5 coefficient of friction on the top of both rails and a 0.2 coefficient of friction on the gage face of the high rail. Simulations meet S-2043 criteria for curving with various lubrication conditions during clockwise runs for this lubrication and profile case and for all runs with other lubrication and profile combinations.

Because there were only small changes to the design of the buffer car since original dynamic predictions were performed, only a small subset of the regimes were run with the revised dynamic model. These regimes were chosen because they allowed for comparison with test data, or because the original dynamic predictions for the regime were close to or did not meet the criteria.

The following table shows a summary of test results and model predictions for the buffer car.

S-2043 Section	Met/Not Met		
	Preliminary Simulations	Revised Simulations	Test Result
5.2 Nonstructural Static Tests			
4.2.1/5.2.1 Truck Twist Equalization	Met	Not Simulated	Met
4.2.2/5.2.2 Carbody Twist Equalization	Met	Not Simulated	Met
4.2.3/5.2.3 Static Curve Stability	Met	Not Simulated	Met
4.2.4/5.2.4 Horizontal Curve Negotiation	Met	Not Simulated	Met
5.4 Structural Tests			
5.4.2 Squeeze (Compressive End) Load	Met	Not Required	Met
5.4.3 Coupler Vertical Loads	Met	Not Required	Met
5.4.4 Jacking	Met	Not Required	Met
5.4.5 Twist	Met	Not Required	Met
5.4.6 Impact	Met	Not Required	Met
5.5 Dynamic Tests			
4.3.11.3/5.5.7 Hunting	Met	Met	Met
4.3.9.6/5.5.8 Twist and Roll	Met	Met	Met
5.5.9 Yaw and Sway	Met	Not Met P-P Lat Accel 1.38 Limit=1.3	Met
5.5.10 Dynamic Curving	Met	Met	Met
4.3.9.7/5.5.11 Pitch and Bounce (Chapter 11)	Met	Met	Met
4.3.9.7/5.5.12 Pitch and Bounce (Special)	Met	Met	Met
4.3.10.1/5.5.13 Single Bump Test	Met	Not Simulated	Met
4.3.11.6/5.5.14 Curve Entry/Exit	Met	Not Simulated	Met
4.3.10.25.5.15 Curving with Single Rail Perturbation	Met	Met	Met
4.3.11.4/5.5.16 Standard Chapter 11 Constant Curving	Met	Not Simulated	Met
4.3.11.7/5.5.17 Special Trackwork	Met	Not Simulated	Met
4.3.11.5 Curving with Various Lubrication Conditions	Met	Not Met Truck Side L/V 0.52, Limit=0.50	Not Required
4.3.12 Ride Quality	Met	Not Simulated	Not Required
4.3.13 Buff and Draft Curving	Not Met Truck Side L/V 0.51, Limit=0.50	Met	Not Required
4.3.14 Braking Effects on Steering	Met	Not Simulated	Not Required
4.3.15 Worn Component Simulations	Met	Not Simulated	Not Required

Table of Contents

1.0 Introduction 1
2.0 Buffer Railcar Description 1
3.0 Objective 3
4.0 Refining the Finite Element Analysis (FEA) 4
4.1 Squeeze (Compressive End) Load 4
4.2 Coupler Vertical Loads 5
4.3 Jacking 6
4.4 Twist 7
4.4.1 Suspension Twist 7
4.4.2 Carbody Twist 8
4.5 Impact Test 9
5.0 New Finite Element Analysis Predictions 10
6.0 Refining the Dynamic Model 10
7.0 New Dynamic Predictions 14
7.1 Twist and Roll 15
7.2 Pitch and Bounce 17
7.3 Special Pitch and Bounce (44.5-foot wavelength) 18
7.4 Yaw and Sway 20
7.5 Dynamic Curving 22
7.6 Curving with a Single-rail Perturbation 24
7.7 Hunting 26
7.8 Curving with Various Lubrication Conditions 27
7.9 Turnouts and Crossovers 29
7.10 Buff and Draft Curving 30
8.0 Conclusions 31
References 33

List of Figures

Figure 1. Buffer railcar IDOX 020001 during static testing 1
Figure 2. Buffer railcar IDOX 020001 arrangement drawing 2
Figure 3. Bearing adapter pad 3
Figure 4. Measurement locations with highest stresses during squeeze (compressive end) load test 5
Figure 5. Measurement locations with highest stresses during coupler vertical load test 6
Figure 6. Measurement locations with highest stresses during jacking test 6
Figure 7. Measurement locations with highest stresses during suspension twist test 8
Figure 8. Measurement locations with highest stresses during carbody twist test 8
Figure 9. Measurement locations with highest stresses during impact test 9
Figure 10. Simulation prediction and test results of minimum vertical wheel load in the twist and roll regime 16
Figure 11. Simulation prediction and test results of peak-to-peak roll angle in the twist and roll regime 17
Figure 12. Simulation prediction and test results of maximum vertical carbody acceleration in the pitch and bounce regime 18
Figure 13. Simulation prediction and test results of maximum vertical carbody acceleration in the special pitch and bounce regime 19
Figure 14. Simulation prediction and test results of maximum peak-to-peak lateral carbody acceleration in the 39-foot wavelength yaw and sway regime 21
Figure 15. Simulation prediction of maximum peak-to-peak lateral carbody acceleration in the 44.5-foot wavelength yaw and sway regime 22
Figure 16. Simulation prediction and test results of maximum wheel l/v ratio in the dynamic curving regime 23
Figure 17. Simulation prediction and test results of minimum vertical wheel load in the dynamic curving regime 24
Figure 18. Simulation prediction and test results of maximum wheel L/V ratio in the curving with 2-inch rail dip regime 25
Figure 19. Simulation prediction and test results of maximum 2,000-foot standard deviation of lateral carbody acceleration in the hunting regime 26
Figure 20. Worn wheel profiles on the ground rail profiles. The wheelset is shifted to the high rail in the position it would be in a left-hand curve 27
Figure 21. Simulation predictions of maximum truck side L/V ratio in the curving with various lubrication conditions regime. Case 2 lubrication with worn profiles 28
Figure 22. Simulation predictions of maximum truck side L/V ratio in the turnouts and crossovers regime 29
Figure 23. Simulation predictions of maximum truck side L/V ratio in the buff and draft curving regime 31

List of Tables

Table 1. Car dimensions 2
Table 2. Buffer car truck configuration 3
Table 3. Comparison of highest measured stresses with predicted stresses for squeeze (compressive end) load test 4
Table 4. Comparison of highest measured stresses with predicted stresses for coupler vertical load test 5
Table 5. Comparison of highest measured stresses with predicted stresses for jacking test 6
Table 6. Comparison of highest measured stresses with predicted stresses for suspension twist test. 7
Table 7. Comparison of highest measured stresses with predicted stresses for carbody twist test 8
Table 8. Comparison of highest measured stresses with predicted stresses for the impact test. 9
Table 9. Comparison of values used in preliminary modeling and values measured during characterization 11
Table 10. Characteristics for original and redesigned spring nest 13
Table 11. Twist and roll test results and simulation predictions 16
Table 12. Pitch and bounce test results and simulation predictions 18
Table 13. Special pitch and bounce test results and simulation predictions 19
Table 14. Yaw and sway (39-foot wavelength) test results and simulation predictions 20
Table 15. Yaw and sway (44.5-foot wavelength) simulation predictions 21
Table 16. Dynamic curving test results and simulation predictions 23
Table 17. Curving with 2-inch rail dip test results and simulation predictions 25
Table 18. Hunting test results and simulation predictions 26
Table 19. Wheel/Rail Coefficients of Friction for the Curving with Various Lubrication Conditions Regime 27
Table 20. Simulation predictions for curving with various lubrication conditions 28
Table 21. Turnout and crossover simulation predictions 29
Table 22. Buff and draft curving simulation predictions 30

1.0 INTRODUCTION

The United States Department of Energy (DOE) contracted with Transportation Technology Center, Inc. (TTCI) to perform dynamic modeling and certification testing on a buffer railcar developed as part of DOE's Atlas Railcar Design Project. The DOE project is intended to meet the needs for future large-scale transport of high-level radioactive material (HLRM) as defined in AAR Standard S-2043, which includes spent nuclear fuel and high-level waste.

All tests and analyses were performed according to the Association of American Railroads' (AAR) *Manual of Standards and Recommended Practices* (MSRP), Standard S-2043, "Performance Specification for Trains used to carry High-level Radioactive Material," Section 5.0 – Single Car Tests.[1] Single-car testing of the buffer railcar was conducted primarily at the U.S. Department of Transportation's Transportation Technology Center (TTC) near Pueblo, Colorado between April 2019 and February 2020. The curving with single-rail perturbation test was repeated on September 11, 2020.

Standard S-2043 requires that structural analysis and dynamic analysis be performed during car design. Kasgro Rail Corporation (Kasgro) designed the car and performed the structural analysis, and TTCI performed the dynamic analysis. Predictions from these analyses are compared to single-car test results in this report. The single-car tests are described in TTCI report P-20-032.[2] The pre-test dynamic analysis is described in TTCI report P-17-023.[3]

2.0 BUFFER RAILCAR DESCRIPTION

The buffer railcar is a four-axle flatcar with a permanently attached ballast load (Figure 1). Kasgro manufactured two prototype buffer cars in 2018, IDOX 020001 and IDOX 020002, which were delivered to the TTC. The tests described in this report were conducted on IDOX 020001. Figure 2 shows the general arrangement drawing of the car. Table 1 shows the car dimensions.



Figure 1. Buffer railcar IDOX 020001 during static testing

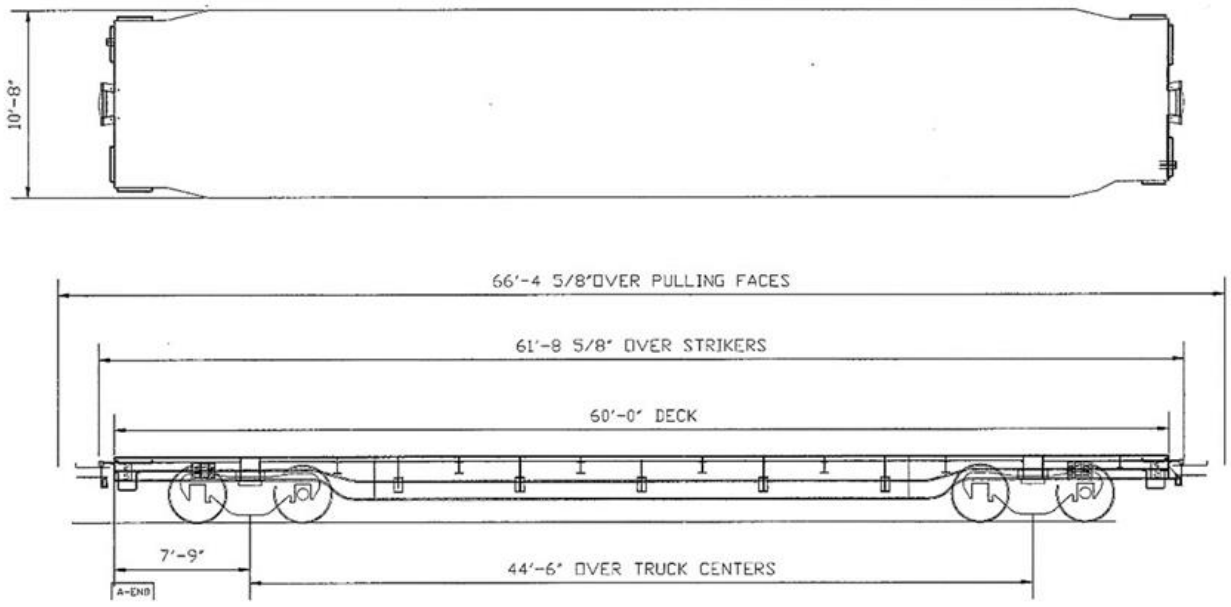


Figure 2. Buffer railcar IDOX 020001 arrangement drawing

Table 1. Car dimensions

Dimension	Value
Length over pulling faces	66 feet, 4 5/8 inches
Length over strikers	61 feet, 8 5/8 inches
Truck center spacing	44 feet 6 inches
Axle spacing on trucks	72 inches

Computer simulations required for Standard S-2043 showed that an empty buffer car would not meet the Standard's requirements in the buff and draft curving regime (S-2043, Paragraph 4.3.13). A ballast weight of 196,000 pounds — included as permanently installed steel plates —was added in the model to resolve this issue.

The steel plates were permanently attached to the car by welding during the manufacturing process, resulting in a car with a permanent gross rail load of 263,000 pounds. Because the car was not rated to carry any additional load, this was the only load condition that was tested.

The car used two Swing Motion® trucks supplied by Amsted Rail. Each truck used two wheelsets having K-axles and AAR1-B narrow flange wheels. Narrow flange wheels were specified for this car because the increased gage clearance allowed more lateral movement for better performance. The trucks were specially designed to use a polymer element between the bearing adapter and side frame. This gave the truck a passive steering capability. Figure 3 shows a bearing adapter pad. Table 2 shows the truck configuration used for testing.



Figure 3. Bearing adapter pad

Table 2. Buffer car truck configuration

Part	Description	
Secondary suspension	Five D7 outer coils, five D6 inner Coils, five D6A inner Coils, two 49427-1, two 49427-2	
Primary suspension	Adapter plus pads, ASF part number 10522A	
Side bearings	Miner TCC-III 60LT	
Friction wedge	Amsted part number 1-9249	
Bearings and adapters	K class 6 1/2 x 9 bearings with 6 1/2 x 9 special adapter ASF Part number 10523A	
Center bowl plate	Metal horizontal liner	
Vertical hydraulic dampers	KONI damper 04a 2032	
Side frames	F9N-10FH-UB	
Bolsters	B9N-714N-FS	
	A-end truck average	B-end truck average
Spring nest height	7.75 inches	7.78 inches
Scale weight	131,200 pounds	131,975 pounds

3.0 OBJECTIVE

The objective of this report is to demonstrate that TTCI compared test results to modeling predictions as part of the structural and dynamic analysis of the DOE buffer car. Where necessary, revised simulation predictions are presented.

4.0 REFINING THE FINITE ELEMENT ANALYSIS (FEA)

Test results are compared to FEA predictions in this section. The FEA results were examined to determine the normal stress in the active direction at the location of the strain gages for comparison to the test results. Paragraph 8.1 of Standard S-2043 requires the following:

> "If any measured stress exceeding 75% of allowable varies from its predicted value by more than 15%, then the model must be refined to provide more accurate predictions."

The results presented in this report show that none of the measured stresses exceed 75 percent of the allowable stress.

4.1 Squeeze (Compressive End) Load

Table 3 provides the summary results from the compressive end load test for the locations with highest measured stress. The locations are highlighted in Figure 4. The maximum measured stress was 60 percent of material yield.

The largest difference between measured and predicted stress for any of the tests was 5.7 ksi (19 percent) on channel SGBF11 during the compressive end load test. Three other measurements in similar locations, (SGBF10, SGBF37, and SGBF35) were closer to the predicted stress.

Table 3. Comparison of highest measured stresses with predicted stresses for squeeze (compressive end) load test

Channel Name	Approximate Location	Measured Stress (ksi)	Yield Stress (ksi)	Measured Stress as percent of Yield	Predicted Stress	Percent Difference Test vs. Predicted
SGBF11	Right edge of bottom flange of center sill, 44.5 inches from A-end body bolster toward car center	-30	50	60%	-24.3	NA*
SGBF10	Left edge of bottom flange of center sill, 44.5 inches from A-end body bolster toward car center	-28	50	56%	-24.3	NA*
SGBF37	Right edge of bottom flange of center sill, 44.5 inches from B-end body bolster toward car center	-26	50	52%	-24.3	NA*
SGDP35	Left edge of bottom flange of center sill, 44.5 inches from B-end body bolster toward car center	-24	50	48%	-24.3	NA*

* Not required because measured stress does not exceed 75% of allowable

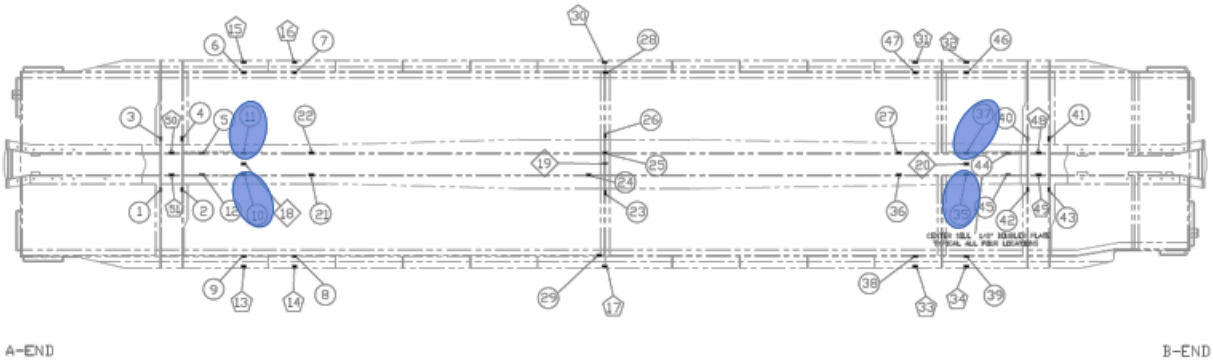


Figure 4. Measurement locations with highest stresses during squeeze (compressive end) load test

4.2 Coupler Vertical Loads

Table 4 shows the summary results from the coupler vertical load test for the locations with highest measured stress. The locations are highlighted in Figure 5. The maximum measured stress was 26% of material yield.

Table 4. Comparison of highest measured stresses with predicted stresses for coupler vertical load test

Channel Name	Approximate Location	Measured Stress (ksi)	Yield Stress (ksi)	Measured Stress as percent of Yield	Predicted Stress	Percent Difference Test vs. Predicted
Load applied upward						
SGBF35	Left edge of bottom flange of center sill, 44.5 inches from B-end body bolster toward car center	12	50	24%	9.3	NA*
SGBF37	Right edge of bottom flange of center sill, 44.5 inches from B-end body bolster toward car center	13	50	26%	9.3	NA*
Load applied downward						
SGBF35	Left edge of bottom flange of center sill, 44.5 inches from B-end body bolster toward car center	-12	50	24%	-8.6	NA*
SGBF37	Right edge of bottom flange of center sill, 44.5 inches from B-end body bolster toward car center	-13	50	26%	-8.6	NA*

* Not required because measured stress does not exceed 75% of allowable

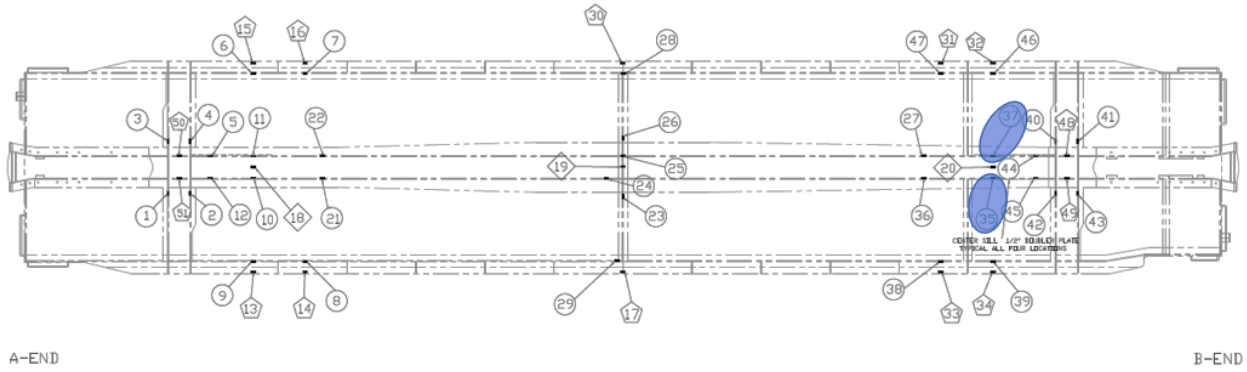


Figure 5. Measurement locations with highest stresses during coupler vertical load test

4.3 Jacking

Table 5 provides the summary results from the jacking test for the locations with highest measured stress. The locations are highlighted in Figure 6. The maximum measured stress was 12 percent of material yield.

Table 5. Comparison of highest measured stresses with predicted stresses for jacking test

Channel Name	Approximate Location	Measured Stress (ksi)	Yield Stress (ksi)	Measured Stress as percent of Yield	Predicted Stress	Percent Difference Test vs. Predicted
SGBF42	Front of bottom flange of B-end body bolster near center sill – left side	6	50	12%	5.3	NA*
SGBF40	Front of bottom flange of B-end body bolster near center sill – right side	6	50	12%	5.3	NA*

* Not required because measured stress does not exceed 75% of allowable

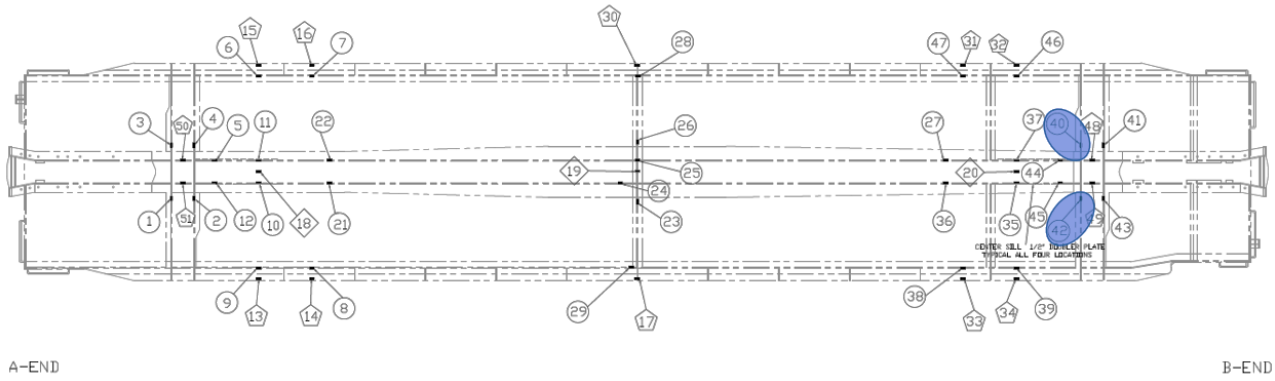


Figure 6. Measurement locations with highest stresses during jacking test

4.4 Twist

TTCI performed two twist tests as part of the structural tests.

The test described in S-2043, Paragraph 5.4.5.1, is reported in Section 4.4.1 of this report, "Suspension Twist." This test followed the requirements of MSRP Section C, Part II, Specification M-1001, Paragraph 11.3.3.5. The test was performed in conjunction with the carbody twist equalization test (S-2043, Paragraph 5.2.2). For this test, two wheels of one side of one truck were raised 3 inches. This was repeated for all four corners of the car.

The test described in S-2043 paragraph 5.4.5.2 is reported in Section 4.4.2 of this report, "Carbody Twist." For this test, the railcar was supported at all four jacking pads and one corner was allowed to drop 3 inches.

4.4.1 Suspension Twist

Table 6 shows the summary results from the suspension twist test for the locations with highest measured stress (locations highlighted in Figure 7). The maximum measured stress was 2 percent of material yield.

Table 6. Comparison of highest measured stresses with predicted stresses for suspension twist test.

Channel Name	Approximate Location	Measured Stress (ksi)	Yield Stress (ksi)	Measured Stress as percent of Yield	Predicted Stress	Percent Difference Test vs. Predicted
Raising wheels A-end left side						
SGDP48	Top of deck plate, longitudinally centered over B-end body bolster, above right edge of center sill	1	50	2%	<1	NA*
Raising wheels A-end right side						
SGDP49	Top of deck plate, longitudinally centered over B-end body bolster, above left edge of center sill	1	50	2%	<1	NA*
Raising wheels B-end left side						
SGDP49	Top of deck plate, longitudinally centered over B-end body bolster, above left edge of center sill	1	50	2%	<1	NA*
Raising wheels B-end right side						
SGDP48	Top of deck plate, longitudinally centered over B-end body bolster, above right edge of center sill	1	50	2%	<1	NA*

* Not required because measured stress does not exceed 75% of allowable

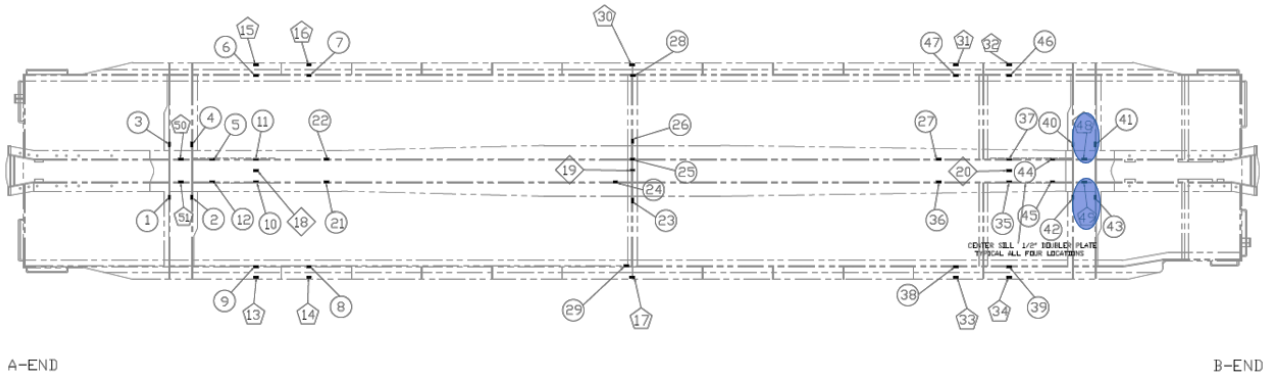


Figure 7. Measurement locations with highest stresses during suspension twist test

4.4.2 Carbody Twist

Table 7 shows the summary results from the carbody twist test for the locations with highest measured stress (locations are highlighted in Figure 8). The maximum measured stress was 18 percent of material yield. The car was supported at three jacking pad locations while the B-end, left-hand jack was lowered to 3 inches. The B-end left jacking pad only dropped 2 11/16 inches, losing contact with the jack.

Table 7. Comparison of highest measured stresses with predicted stresses for carbody twist test

Channel Name	Approximate Location	Measured Stress (ksi)	Yield Stress (ksi)	Measured Stress as percent of Yield	Predicted Stress	Percent Difference Test vs. Predicted
SGBF11	Right edge of bottom flange of center sill, 44.5 inches from A-end body bolster toward car center	-3	50	6%	-5	NA*
SGBF40	Front of bottom flange of B-end body bolster near center sill – right side	8	50	18%	7.4	NA*

* Not required because measured stress does not exceed 75% of allowable

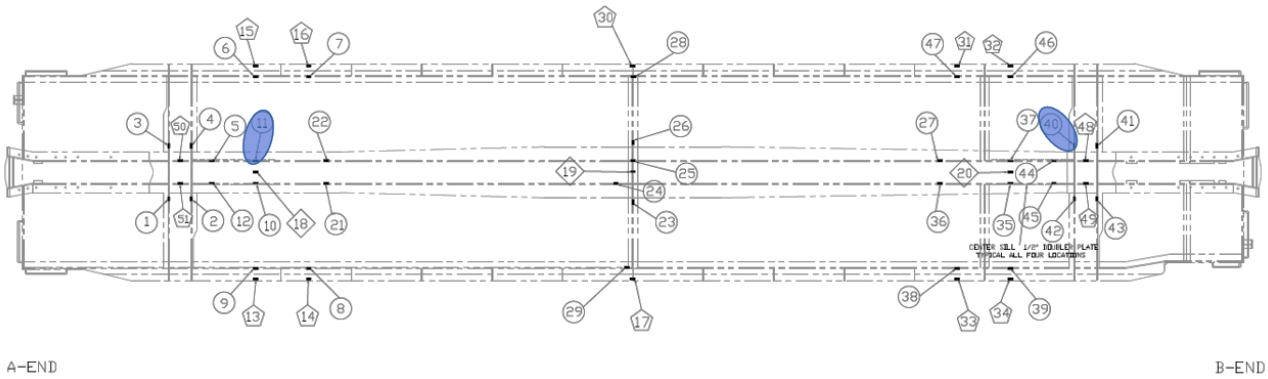


Figure 8. Measurement locations with highest stresses during carbody twist test

4.5 Impact Test

Table 8 shows the summary results from the impact test for the locations with highest measured stress (locations are highlighted in Figure 9). The highest stresses were measured at the highest impact speed of 9.6 mph. The coupler load measured on this run was 612 kips. The maximum measured stress was 32 percent of material yield.

Table 8. Comparison of highest measured stresses with predicted stresses for the impact test.

Channel Name	Approximate Location	Measured Stress (ksi)	Yield Stress (ksi)	Measured Stress as percent of Yield	Predicted Stress	Percent Difference Test vs. Predicted
SGBF37	Right edge of bottom flange of center sill, 44.5 inches from B-end body bolster toward car center	-16	50	32%	-16.5	NA*
SGBF35	Left edge of bottom flange of center sill, 44.5 inches from B-end body bolster toward car center	-14	50	28%	-16.5	NA*
SGBF44	Right edge of bottom flange of center sill, 18.75 inches from B-end body bolster toward car center	-9	50	18%	-9.76	NA*
SGBF45	Left edge of bottom flange of center sill, 18.75 inches from B-end body bolster toward car center	-9	50	18%	-9.76	NA*

* Not required because measured stress does not exceed 75% of allowable

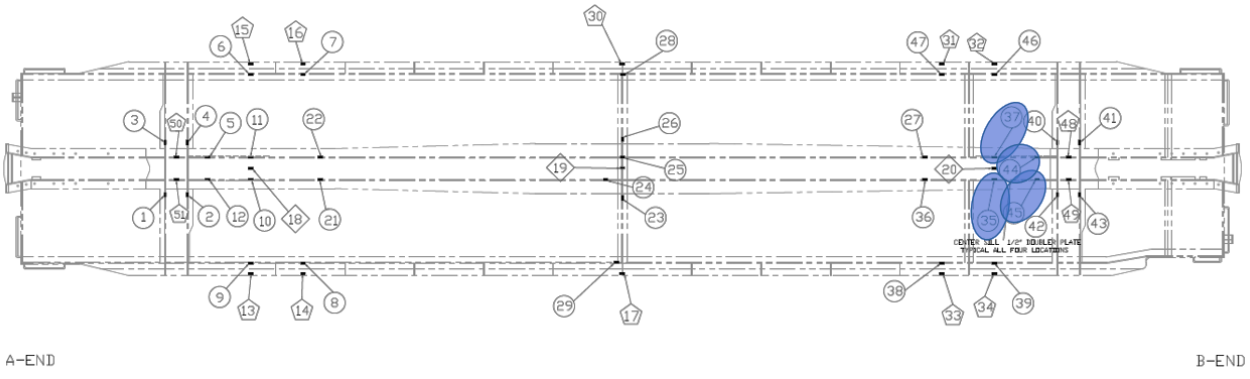


Figure 9. Measurement locations with highest stresses during impact test

5.0 NEW FINITE ELEMENT ANALYSIS PREDICTIONS

Because none of the measured stresses were greater than 75 percent of the allowable stress, the tolerance on FEA prediction accuracy did not apply. No new FEA predictions were required.

6.0 REFINING THE DYNAMIC MODEL

Standard S-2043 requires:

> "The dynamic model must be refined based on vehicle characterization results if suspension values are measurably different than those used in the original model."

Some of the measured characterization results[2] differ from those used in the original dynamic analysis model.[3] Table 9 provides the suspension stiffness and damping values used for the original model, the values measured during the characterization, the percent difference, information on the origin of the characterization value, and an indication if and how the characterization value was used to update the model.

Table 9. Comparison of values used in preliminary modeling and values measured during characterization

Parameter	Model Value	Characterization Value	Percent Difference	Notes	Change to model
Spring vertical stiffness (pound/inch/nest)*	22,400	23,600	5%	Spring nest stiffness compiled using the manufacturer / AAR values compared to values measured during component characterization	Updated for the appropriate spring group
Vertical secondary stiffness (pound/inch/nest)*	22,400	26,000	16%	Manufacturer / AAR values of original nest compared to System Characterizations values measured on the MSU, dampers removed.	Besides changing to the correct spring group, no change was made
Lateral secondary stiffness (pound/inch/nest)*	13,500	8,100	-40%	Average transom restrained; wedges installed runs	Reduced stiffness to 62% of Koffman formula
Vertical secondary damping (pound/nest)	8,000	5,000	-38%	Dampers removed	No change made
Lateral secondary damping (pound/nest)	9,000	6,000	-33%	Average transom restrained; wedges installed runs	No change made
Side bearing preload (pounds)**	7,500	5,700	-24%	Manufacturers static closure compared to average from component characterization	Updated the model to use a Piece Wise Linear (PWL) value based on the characterization data of the side bearing used
Center plate friction (nondimensional)	0.2	0.22	10%		Increased stiffness to characterization value
Damper initial rate (pound/(inch/second))	1070	1054	-1%	Slope of data from -4 inch/second to 4 inch/second	No Change
Damper blowoff velocity (inch/second)	3.94	3.98	1%	Intersection of initial rate line and damper blowoff lines	No Change
Damper blowoff rate(pound/(inch/second)	58	58	0%	Slope of data from -14 to -4 inch/second averaged with slope of data from 4 to 14 inches/second	No Change
Damper bushing series stiffness (pound/inch)	71,377	102,000	43%	Average of series stiffness of AL and AR dampers	Increased the damper bushing series stiffness to the characterization level
Vertical primary stiffness (pound/inch/pad)	500,000	850,000	70%	0.1Hz data. Data varied over a range from 763,000 to 923,000	Increased stiffness to the characterization value
Lateral primary stiffness	48,000	33,500	-30%	0.1Hz data. Data varied over a range	Reduced stiffness to characterization

Parameter	Model Value	Characterization Value	Percent Difference	Notes	Change to model
(pound/inch/pad)				from 30,000-to 37,000	value
Longitudinal primary stiffness at axle centerline (pound/inch/pad)	22,500	13,000	-42%	Average of axle centerline stiffness measured directly and derived from yaw	Reduced stiffness to characterization value

* The original model used 6 D7 OC and 6 D7 IC, during production the truck design was changed to use 5 D7 OC, 5 D6 IC, and 5 D6A IIC as described below

** The model used Miner TCC III 8000 CCSB, during production the car design was changed to use Miner TCC III 6000 CCSB as described below

The original simulation predictions were performed with a spring nest configuration containing six D7 outer coils, six D7 inner coils, two 49427-1 outer control coils, two 49427-2 inner control coils, and a KONI vertical damper. Amsted Rail later determined that this spring nest was not compatible with the KONI Damper because the six-coil nest did not allow enough space to install the damper. To provide space, Amsted Rail redesigned the spring nest to use five D7 outer coils, five D6 inner coils, five D6A inner-inner coils, two 49427-1 outer control coils and two 49427-2 inner control coils. Table 10 shows characteristics for the original and redesigned spring nests.

Table 10. Characteristics for original and redesigned spring nest

Metric	Spring Nest - Original Simulation Predictions	Redesigned Spring Nest
Reserve capacity (percent)	57	54
Load on a single wedge (pound)	6,486	6,870
Total lateral stiffness per nest (pound/inch)	13,509	13,030
Total vertical stiffness per nest (pound/inch)	22,412	23,788
Static free height (inch)	8.13	7.95

A second change to the buffer car equipment was the four constant-contact side bearings mounted between the truck bolsters and carbody bolsters. The dynamic analysis model used characteristics for a Miner TCC-III 80 LT side bearing. The prototype cars arrived with Miner TCC-III 60 LT side bearings installed. The TCC-III 80 LT side bearings have a nominal preload of 8,000 pounds while the TCC-III 60 LT side bearings have a nominal preload of 6,000 pounds. Two of the TCC-III 60 LT side bearings were characterized. The force deflection data from the characterization was used in the refined dynamic model.

The lateral secondary suspension stiffness measured during the characterization test was only about 60 percent of the value used in the dynamic analysis model. Part of this difference was due to the change in the secondary suspension spring group. A larger part of the difference was that the formula used to estimate the shear stiffness often predicts a higher stiffness than is found in practice. The shear stiffness in the revised dynamic model was calculated for the redesigned spring group, and then reduced to 62 percent of the calculated value to match the value from characterization tests.

The original dynamic analysis model used a coefficient of friction value of 0.2 to model the surface between the carbody center plate and the truck center bowl. The coefficient of friction measured during the characterization test was 0.22. The refined dynamic model used a coefficient of friction of 0.22 for this surface.

The characterization data for the KONI vertical damper matched the values used in the dynamic analysis model very closely for the initial rate, blowoff velocity, and the blowoff rate. TTCI made no changes in the refined model for these parameters. The vertical damper bushing stiffness measured during the characterization was about 30 percent higher than the value in the original dynamic analysis model. The bushing stiffness was increased to match the characterization data for the refined dynamic analysis model.

The measured stiffness of the primary suspension pads was different than those used in the original dynamic analysis model. The measured vertical stiffness was 41 percent higher while the

lateral and longitudinal stiffness were 43 and 73 percent lower, respectively. These values of primary suspension pad stiffness were updated to match the characterization values in the refined dynamic analysis model.

While troubleshooting performance of a similar truck design in the time since the original dynamic analysis was performed, TTCI found that the method used to model the connection between the side frame and the primary pad could be altered to better replicate the roll characteristics between the side frame and axle. The original method to model this connection used only a single vertical connection between the side frame and axle centered at the location of the primary pad. When comparing predicted lateral suspension displacement to test results, TTCI found that the results matched better when two connections — separated laterally the width of the primary pad — were used to model this connection. This new method was implemented in the refined dynamic analysis model.

7.0 NEW DYNAMIC PREDICTIONS

Standard S-2043 states the following:

> "Test results must be compared to design predictions to verify that the model accurately represents the vehicle. If substantial modifications have been made to the dynamic model, a revised analysis must be performed. The designer may choose to repeat the entire analysis or reanalyze limited cases based on how critically they would be affected by the changes to the model and how large existing margins of safety are. The designer's decisions must be justified through adequate explanation."

In this section, TTCI compares original and refined dynamic analysis model predictions to test data to show that the model accurately represents the vehicle. Characterization test results prompted several changes to the dynamic analysis model. As a result, TTCI repeated several portions of the dynamic analysis. Simulation predictions are shown for the original and revised models.

TTCI repeated the following portions of the dynamic analysis because they served to demonstrate the model performance compared to test data:

- Twist and roll
- Pitch and bounce
- Yaw and sway
- Dynamic curving
- Curving with single rail perturbation
- Hunting

TTCI repeated the following portions of the dynamic analysis because the original dynamic analysis predictions showed that some metrics were close to or did not meet the criteria.

- Curving with various lubrication conditions
- Turnouts and crossovers
- Buff and draft curving

As will be shown in the following sections, the revised model predictions for the regimes listed above changed very little compared to the original dynamic analysis. Because the revised model showed little change compared to the original model, and because the original dynamic analysis

showed a margin of safety with respect to the criteria for these regimes, the regimes below were not simulated with the revised model:

- Twist and roll – 44.5-foot
- Yaw and sway – 44.5-foot
- Dynamic curve – 44.5-foot
- Single bump
- Constant curving
- Limiting spiral negotiation
- Ride quality
- Braking effects on steering
- Worn component simulations

The proceeding sections show modeling predictions for the original model, the revised model, and test results where available. The buffer car met all the single-car test requirements. The original dynamic analysis predictions met all the requirements except for two of the curving with various lubrication conditions and buff-draft curving requirements.

7.1 Twist and Roll

Simulations of the twist and roll regime were conducted according to Standard S-2043, Paragraph 4.3.9.6. Twist and roll track tests were conducted according to S-2043, Paragraph 5.5.8. The twist and roll regime consists of a series of 10 0.75-inch vertical track deviations offset on each rail to input roll motions to the car. The original simulations were performed with 39- and 44.5-foot wavelengths. Track tests were only performed with 39-foot wavelength. Simulations with a 44.5-foot wavelength were not performed with the revised model because there were no test results for comparison and the original simulations showed a large margin of safety compared to the criteria.

Table 11 shows the worst-case test results and simulation predictions for twist and roll. Figure 10 shows minimum vertical wheel load and Figure 11 shows the maximum peak-to-peak roll angles plotted against speed to show the trend in performance. Test results and simulation predictions met S-2043 criteria (red line) for twist and roll. The Chapter 11 criteria (yellow line) is also shown as reference.

Simulation predictions and test results matched closely for twist and roll. Test results showed lower wheel loads than simulation predictions at speeds above 30 mph, but at the widest point the difference is only about 8 percent of static wheel load. Peak-to-peak carbody roll angle test results showed a mild lower center roll resonance at about 30 mph for the old and new model predictions and at about 33 mph for the test. Peak-to-peak carbody roll angle test results showed a mild upper center roll resonance at about 65 mph for the old model predictions and at about 60 mph for the new model predictions and the test. The upper center roll peak was slightly more pronounced for the revised model predictions than the test data, but it occurred at the same speed and was followed by a similar reduction in amplitude at the higher speeds.

Table 11. Twist and roll test results and simulation predictions

Criterion	Limiting Value	Test Result	Simulation Prediction Original Model	Simulation Prediction Revised Model
Roll angle (degree)	4.0	1.7	1.6	2.1
Maximum wheel lateral/vertical (L/V)	0.8	0.2	0.11	0.19
Maximum truck side L/V	0.5	0.16	0.09	0.13
Minimum vertical wheel load (%)	25%	66%	69%	69%
Lateral peak-to-peak acceleration (g)	1.3	0.55	0.27	0.34
Maximum lateral acceleration (g)	0.75	0.31	0.15	0.20
Maximum vertical acceleration (g)	0.90	0.29	0.16	0.23
Maximum vertical suspension deflection (%)	95%	48%	40%	46%

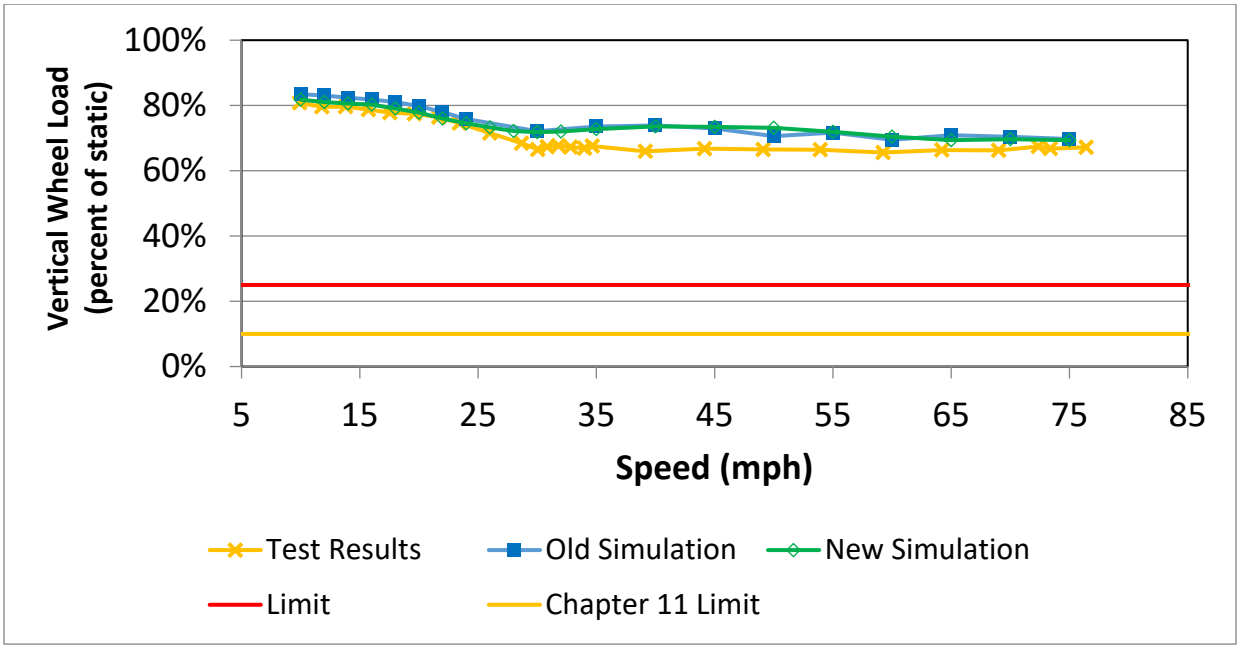


Figure 10. Simulation prediction and test results of minimum vertical wheel load in the twist and roll regime

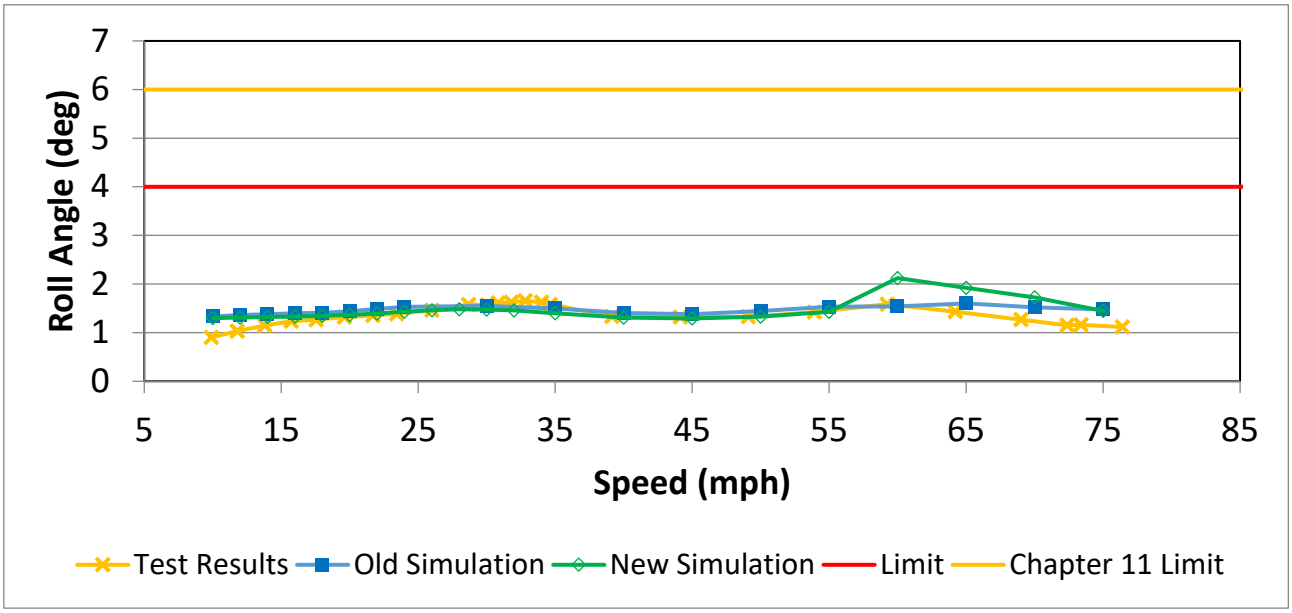


Figure 11. Simulation prediction and test results of peak-to-peak roll angle in the twist and roll regime

7.2 Pitch and Bounce

Simulations of the pitch and bounce regime were conducted according to S-2043, Paragraph 4.3.9.7. Pitch and bounce tests were conducted according to of S-2043, Paragraph 5.5.11. The pitch and bounce regime consisted of a series of 10 0.75-inch vertical track deviations in parallel on each rail to input vertical motions to the car.

Table 12 shows the worst-case test results and simulation predictions for pitch and bounce. Figure 12 shows the maximum carbody vertical acceleration plotted against speed to show the trend in performance. Test results and simulation predictions met S-2043 criteria for pitch and bounce.

Simulation predictions showed lower amplitude resonance at a slightly lower speed than test results for pitch and bounce. For example, the original simulation predicted the maximum carbody vertical acceleration of 0.65 g at about 59 mph; for the refined simulation, the prediction increased to 0.68 g at about 60 mph and the test result showed 0.8 g at 68 mph. The changes to the model that represented the new spring grouping improved the simulation predictions slightly, but there was still a difference when compared to the test results.

Table 12. Pitch and bounce test results and simulation predictions

Criterion	Limiting Value	Test Result	Simulation Prediction Original Model	Simulation Prediction Revised Model
Roll angle (degree)	4.0	0.4	0.2	0.3
Maximum wheel L/V	0.8	0.19	0.06	0.07
Maximum truck side L/V	0.5	0.13	0.05	0.06
Minimum vertical wheel load (%)	25%	50%	60%	59%
Lateral peak-to-peak acceleration (g)	1.3	0.31	0.12	0.15
Maximum lateral acceleration (g)	0.75	0.25	0.06	0.08
Maximum vertical acceleration (g)	0.90	0.80	0.65	0.68
Maximum vertical suspension deflection (%)	95%	86%	74%	75%

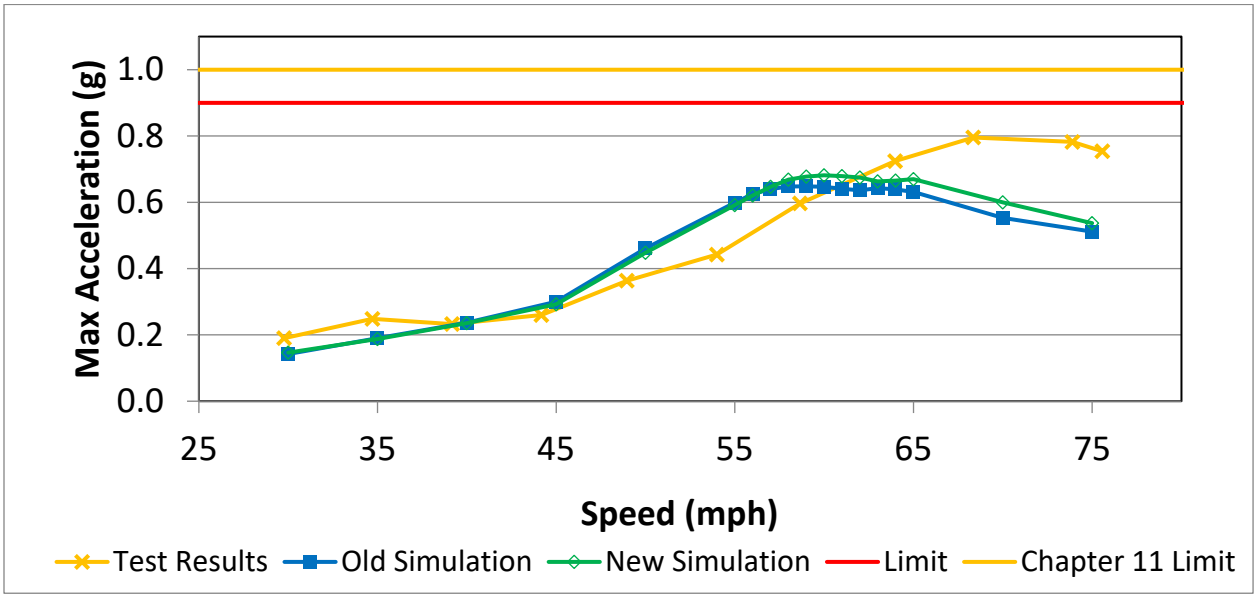


Figure 12. Simulation prediction and test results of maximum vertical carbody acceleration in the pitch and bounce regime

7.3 Special Pitch and Bounce (44.5-foot wavelength)

Simulations of the special pitch and bounce regime (44.5-foot wavelength) were conducted according to S-2043, Paragraph 4.3.9.7. Special pitch and bounce tests were conducted according to S-2043, Paragraph 5.5.12. The special pitch and bounce regime consisted of a series of 10 0.75-inch vertical track deviations in parallel on each rail to input vertical motions to the car. The difference between standard Chapter 11 pitch and bounce and special pitch and bounce is that the standard zone uses track deviations on a 39-foot wavelength while the special zone uses track deviations on a wavelength that matches the truck center spacing of the car being tested — 44.5 feet in this case.

Table 13 shows the worst-case test results and simulation predictions for special pitch and bounce. Figure 13 shows the maximum carbody vertical acceleration plotted against speed to show the trend in performance. Test results and simulation predictions meet S-2043 criteria for special pitch and bounce.

Simulation predictions showed lower amplitude resonance at a slightly lower speed than test results for pitch and bounce. For example, the original simulation predicted the maximum carbody vertical acceleration of 0.47 g at about 60 mph; for the refined simulation, the prediction increased to 0.49 g at about 61 mph, and the test result showed 0.5 g at 69 mph. The changes to the model that represented the new spring grouping improved the simulation predictions slightly, but there was still a difference when compared to the test results.

The simulation predictions did correctly predict the improvement in performance in the special pitch and bounce regime compared to the standard pitch and bounce regime. Minimum vertical wheel loads increased for both the simulation and test in the special pitch and bounce compared to standard pitch and bounce. Maximum carbody acceleration and maximum vertical suspension deflection both decreased for both the simulation and test in the special pitch and bounce compared to standard pitch and bounce.

Table 13. Special pitch and bounce test results and simulation predictions

Criterion	Limiting Value	Test Result	Simulation Prediction Original Model	Simulation Prediction Revised Model
Roll angle (degree)	4.0	0.4	0.2	0.2
Maximum wheel L/V	0.8	0.13	0.08	0.07
Maximum truck side L/V	0.5	0.09	0.06	0.06
Minimum vertical wheel load (%)	25%	57%	65%	64%
Lateral peak-to-peak acceleration (g)	1.3	0.22	0.19	0.17
Maximum lateral acceleration (g)	0.75	0.18	0.12	0.09
Maximum vertical acceleration (g)	0.90	0.5	0.47	0.49
Maximum vertical suspension deflection (%)	95%	71%	61%	61%

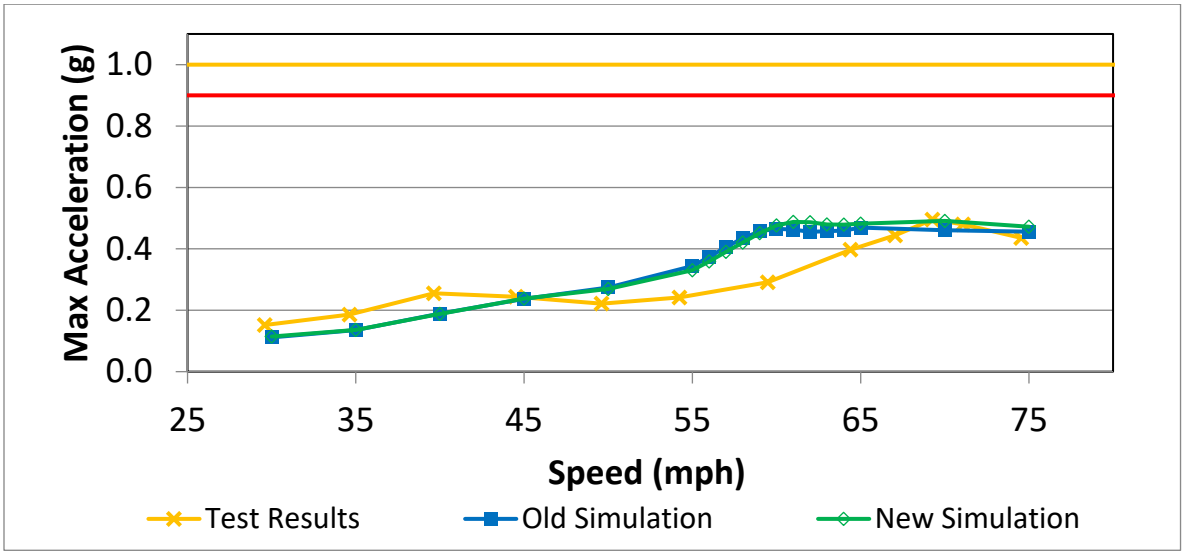


Figure 13. Simulation prediction and test results of maximum vertical carbody acceleration in the special pitch and bounce regime

7.4 Yaw and Sway

Simulations of the yaw and sway regime were conducted according to S-2043, Paragraph 4.3.9.8. Yaw and sway tests were conducted according to S-2043, Paragraph 5.5.9. The yaw and sway regime consisted of a series of five 1.25-inch lateral track deviations on a section with 1-inch wide gage to input lateral and yaw motions to the car. Simulations of 39-foot and 44-foot, 6-inch wavelengths were performed. Testing was carried out with 39-foot wavelength only.

Table 14 shows the worst-case test results and simulation predictions for yaw and sway with 39-foot wavelength. Figure 14 shows the maximum peak-to-peak carbody lateral acceleration plotted against speed to show the trend in performance. Table 15 shows the worst-case simulation predictions for yaw and sway with 44.5-foot wavelength. Figure 15 shows the maximum peak-to-peak carbody lateral acceleration plotted against speed to show the trend in performance. Test results and the original simulation predictions met S-2043 criteria for yaw and sway, but the revised simulation predictions did not meet S-2043 criteria for yaw and sway at speeds between 30 and 35 mph. The revised simulation predictions did meet the slightly less stringent Chapter 11 criteria.

The simulation predictions had a higher amplitude resonance at a lower critical speed that was measured during the test. Unfortunately, the revised model exacerbated this problem by increasing the amplitude of the resonance further, to the point that the simulation predictions no longer met the criteria for yaw and sway.

Table 14. Yaw and sway (39-foot wavelength) test results and simulation predictions

Criterion	Limiting Value	Test Result	Simulation Prediction Original Model	Simulation Prediction Revised Model
Roll angle (degree)	4.0	2.0	1.3	2.3
Maximum wheel L/V	0.8	0.6	0.62	0.62
Maximum truck side L/V	0.5	0.3	0.30	0.29
Minimum vertical wheel load (%)	25%	50%	56%	52%
Lateral peak-to-peak acceleration (g)	1.3	0.9	1.16	**1.38**
Maximum lateral acceleration (g)	0.75	0.5	0.59	0.70
Maximum vertical acceleration (g)	0.90	0.3	0.18	0.18
Maximum vertical suspension deflection (%)	95%	67%	77%	46%

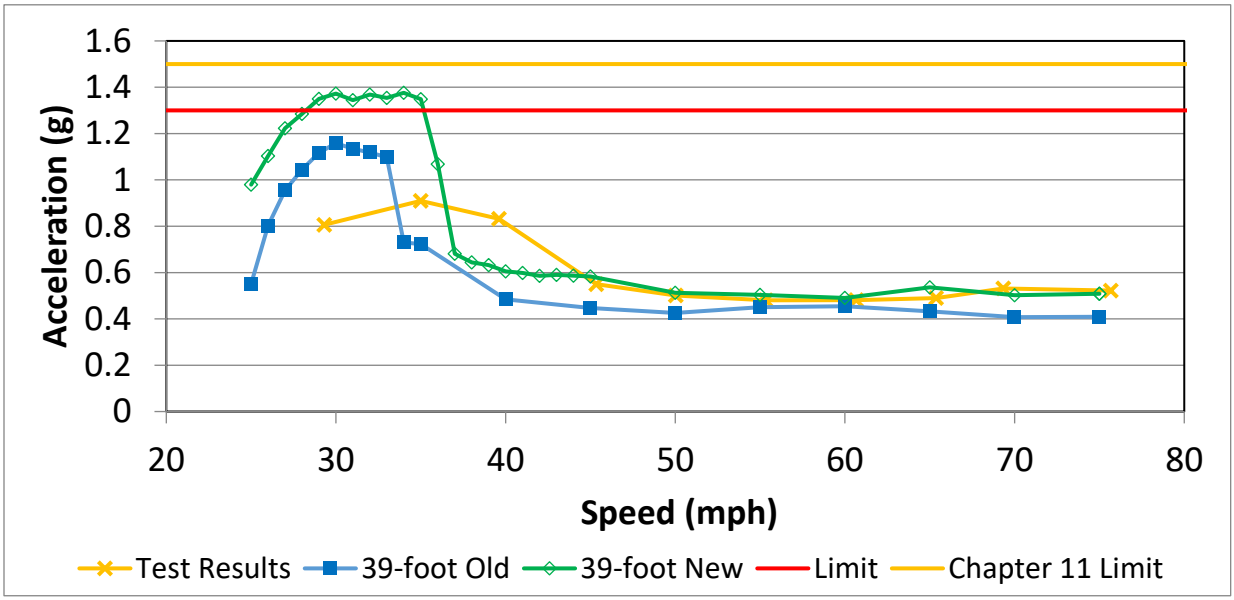


Figure 14. Simulation prediction and test results of maximum peak-to-peak lateral carbody acceleration in the 39-foot wavelength yaw and sway regime

Table 15. Yaw and sway (44.5-foot wavelength) simulation predictions

Criterion	Limiting Value	Simulation Prediction Original Model	Simulation Prediction Revised Model
Roll angle (degree)	4.0	2.0	3.3
Maximum wheel L/V	0.8	0.51	0.47
Maximum truck side L/V	0.5	0.24	0.23
Minimum vertical wheel load (%)	25%	51%	50%
Lateral peak-to-peak acceleration (g)	1.3	1.25	**1.31**
Maximum lateral acceleration (g)	0.75	0.65	0.68
Maximum vertical acceleration (g)	0.90	0.16	0.17
Maximum vertical suspension deflection (%)	95%	79%	49%

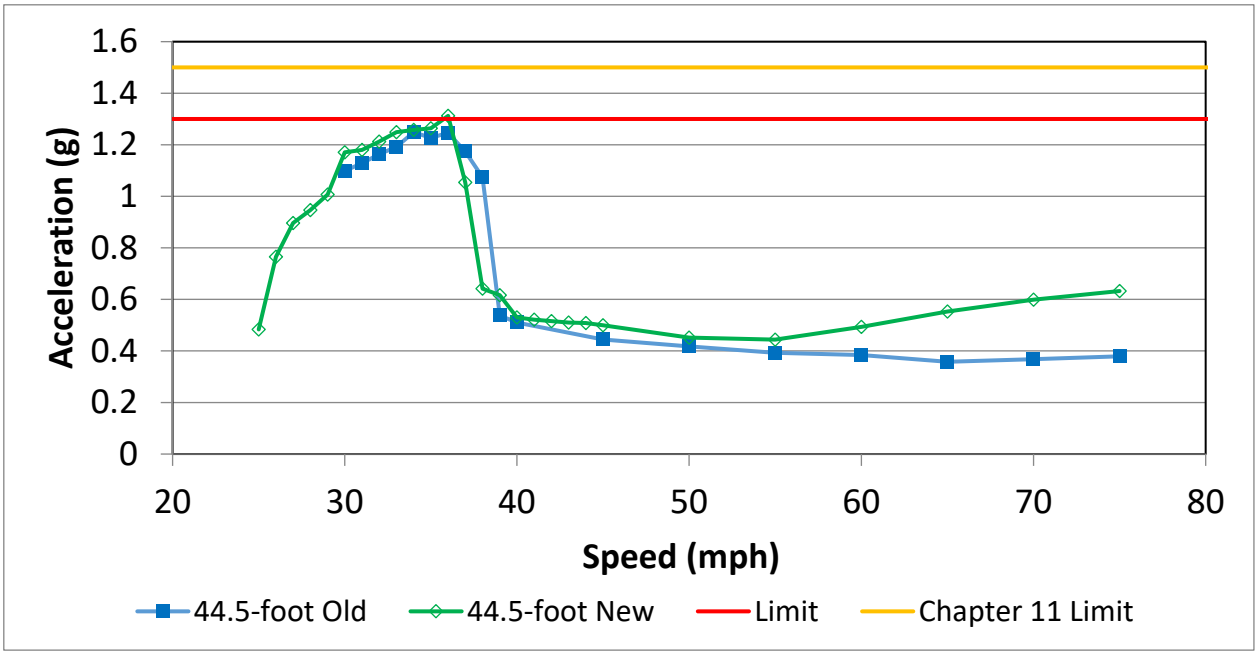


Figure 15. Simulation prediction of maximum peak-to-peak lateral carbody acceleration in the 44.5-foot wavelength yaw and sway regime

7.5 Dynamic Curving

Simulations of the dynamic curving regime were conducted according to Paragraph 4.3.9.9 of S-2043. Dynamic curving tests were conducted according to Paragraph 5.5.10 of S-2043. The dynamic curve section was on a 10-degree curve with 4 inches superelevation. The dynamic curving regime consisted of a series of 0.5-inch vertical track deviations offset on each rail to input roll motions to the car. There were five deviations on the high rail and six deviations on the low rail. At the same time, the gage of the track changed from 56.5 inches to 57.5 inches to input lateral motions to the car. Simulations of 39-foot and 44-foot 6-inch wavelengths were performed at speeds ranging from 10 mph to 32 mph (3 inches of cant deficiency) in increments of 2 mph or less.

Table 16 shows the worst-case test results and simulation predictions for dynamic curving with 39-foot wavelength. Figure 16 shows the maximum wheel L/V ratio and Figure 17 shows minimum vertical wheel load plotted against speed to show the trend in performance. Test results and the simulation predictions met S-2043 criteria for dynamic curving.

Simulations predict slightly lower L/V ratios and slightly higher vertical wheel loads that were measured in the test for dynamic curving. The revised model improved the comparisons slightly for most metrics.

The models show the correct trends with speed compared to test data. Figure 16 shows the maximum wheel L/V ratio is steady across the speed range. Figure 17 shows the minimum vertical wheel holds steady from 10 mph to about 20 mph and then begins to drop off. The test results showed the drop in vertical wheel loads becomes steeper at 30 and 32 mph while the model predicted wheel loads continue to drop at the same rate.

Table 16. Dynamic curving test results and simulation predictions

Criterion	Limiting Value	Test Result	Simulation Prediction Original Model	Simulation Prediction Revised Model
Roll angle (degree)	4.0	1.4	1.0	1.0
Maximum wheel L/V	0.8	0.66	0.53	0.55
Maximum truck side L/V	0.5	0.45	0.25	0.28
Minimum vertical wheel load (%)	25%	34%	62%	58%
Lateral peak-to-peak acceleration (g)	1.3	0.96	0.41	0.67
Maximum lateral acceleration (g)	0.75	0.69	0.28	0.47
Maximum vertical acceleration (g)	0.90	0.16	0.09	0.11
Maximum vertical suspension deflection (%)	95%	42%	33%	34%

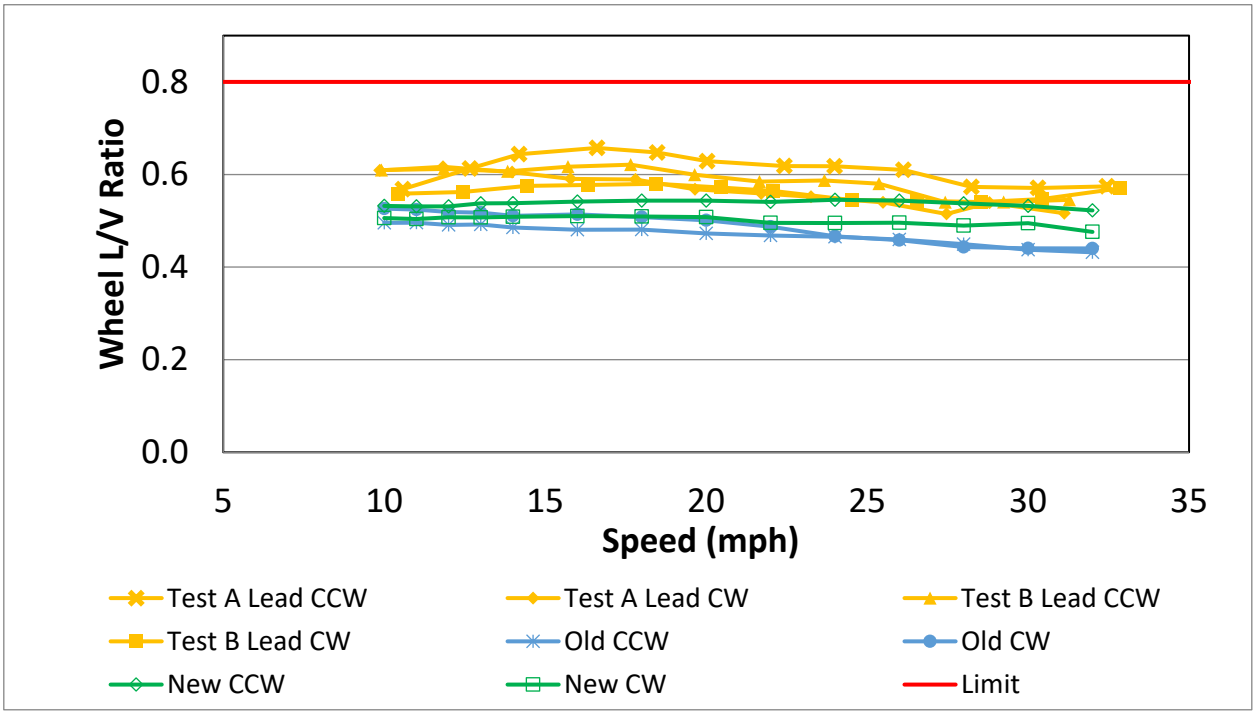


Figure 16. Simulation prediction and test results of maximum wheel l/v ratio in the dynamic curving regime

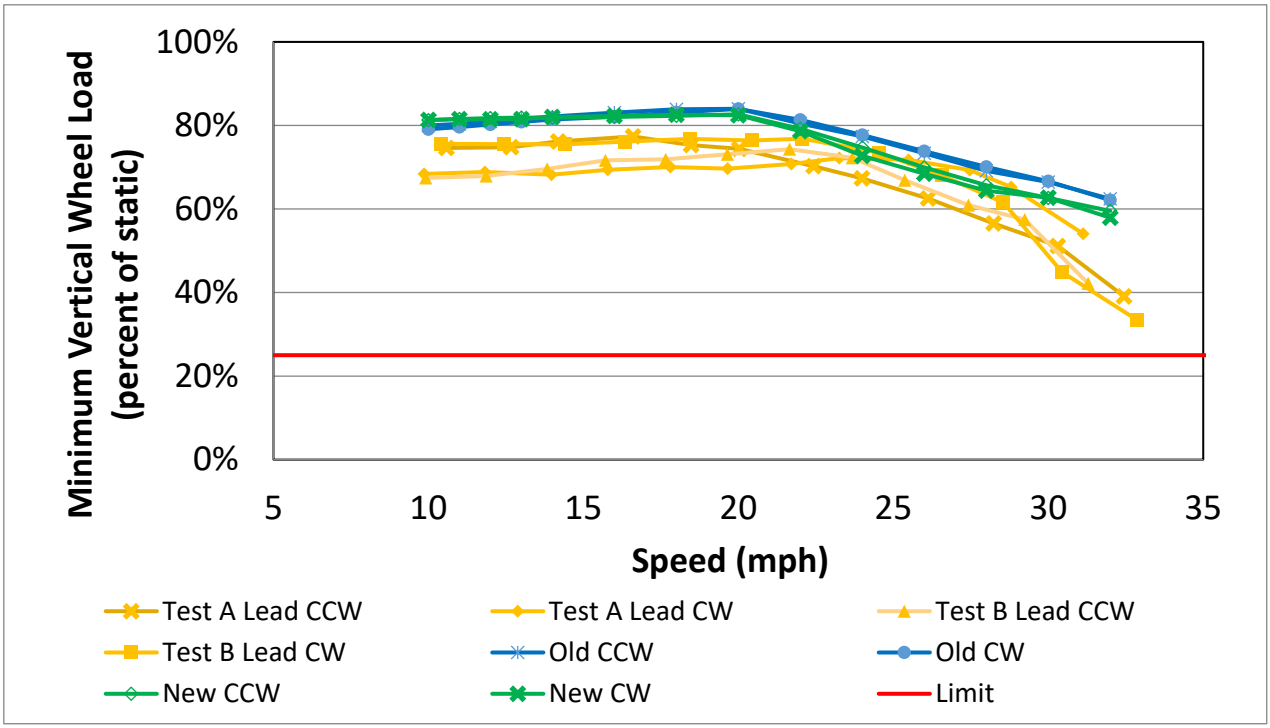


Figure 17. Simulation prediction and test results of minimum vertical wheel load in the dynamic curving regime

7.6 Curving with a Single-rail Perturbation

Simulations of the curving with a single-rail perturbation regime were conducted according to S-2043, Paragraph 4.3.10.2. Curving with single rail perturbation tests were conducted according to S-2043, Paragraph 5.5.15. Simulations were made for 1-, 2-, and 3-inch outside rail dips and 1-, 2-, and 3-inch inside rail bumps in a 12-degree curve with zero superelevation, but only data for the 2-inch dip perturbations are presented here. The inside rail bump was a flat-topped ramp with an elevation change over 6 feet, a steady elevation over 12 feet, ramping back down over 6 feet. The outside rail dip was the reverse. Tests were performed with 2-inch amplitude perturbations. The outside rail dip predictions and test results are presented here because the dip section was the most severe condition for both simulations and tests.

Table 17 shows the worst-case test results and simulation predictions for curving with single rail perturbation with a 2-inch dip. Figure 18 shows the maximum wheel L/V ratio plotted against speed to show the trend in performance. Test results and the simulation predictions met S-2043 criteria for curving with single rail perturbations.

Figure 18 shows that the original simulations predictions matched test results more closely than the revised simulations for test data with A-end lead in the clockwise direction, A-end lead in the counterclockwise direction, and B-end lead in the counterclockwise direction. The revised simulation predictions more closely match the test data with B-end lead in the clockwise direction.

Table 17. Curving with 2-inch rail dip test results and simulation predictions

Criterion	Limiting Value	Test Result	Simulation Prediction Original Model	Simulation Prediction Revised Model
Roll angle (degree)	4.0	1.4	1.7	2.0
Maximum wheel L/V	0.8	0.70	0.57	0.50
Maximum truck side L/V	0.5	0.36	0.29	0.22
Minimum vertical wheel load (%)	25%	60%	67%	65%
Lateral peak-to-peak acceleration (g)	1.3	0.17	0.11	0.13
Maximum lateral acceleration (g)	0.75	0.13	0.07	0.09
Maximum vertical acceleration (g)	0.90	0.18	0.11	0.08
Maximum vertical suspension deflection (%)	95%	68%	35%	37%

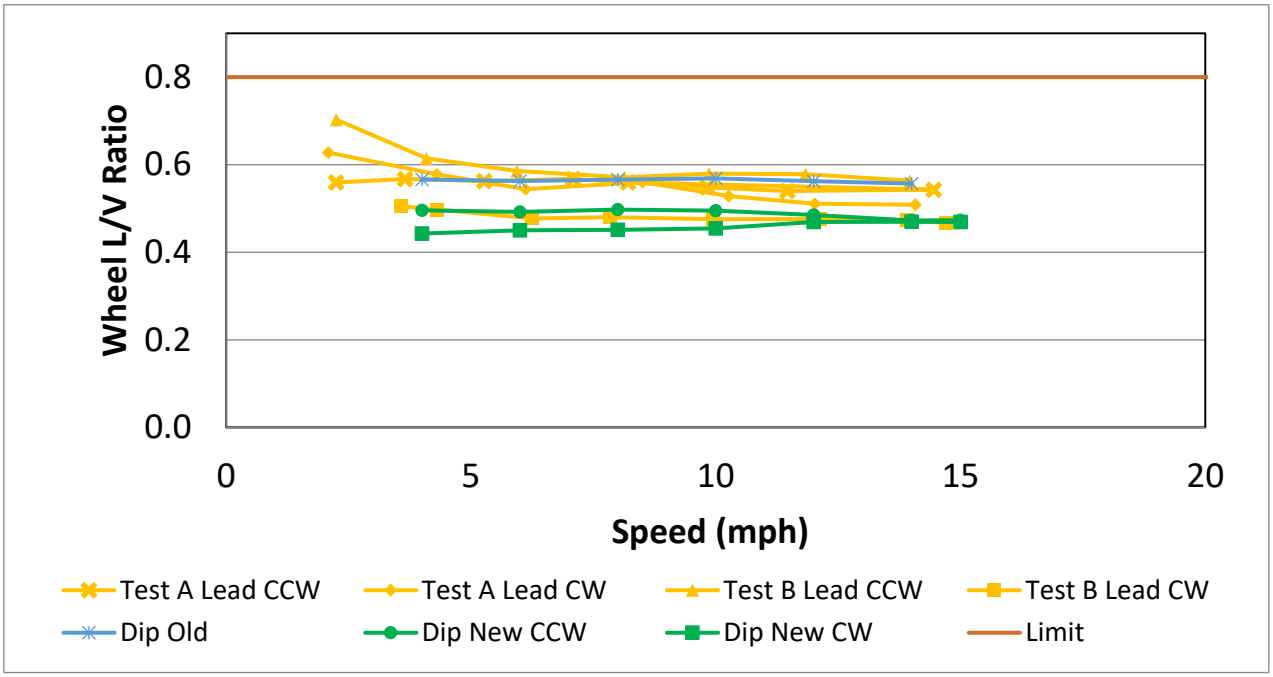


Figure 18. Simulation prediction and test results of maximum wheel L/V ratio in the curving with 2-inch rail dip regime

7.7 Hunting

Simulations of the hunting regime were conducted according to S-2043, Paragraph 4.3.11.3.1. Hunting tests were conducted according to S-2043, Paragraph 5.5.7. Simulations used inputs from measured track geometry of the test site, a 5,500-foot section of tangent track on the TTC Railroad Test Track.

Table 18 shows the worst-case test results and simulation predictions for hunting with a 2-inch dip. Figure 19 shows the 2,000-foot standard deviation of lateral carbody acceleration plotted against speed to show the trend in performance. Test results and the simulation predictions met S-2043 criteria for hunting.

Table 18. Hunting test results and simulation predictions

Criterion	Limiting Value	Test Result	Simulation Prediction Original Model	Simulation Prediction Revised Model
Roll angle (degree)	4.0	0.7	0.4	0.3
Maximum wheel L/V	0.8	*	0.21	0.12
Maximum truck side L/V	0.5	*	0.19	0.10
Minimum vertical wheel load (%)	25%	*	66%	80%
Lateral peak-to-peak acceleration (g)	1.3	0.37	0.41	0.34
Maximum lateral acceleration (g)	0.75	0.20	0.30	0.18
Lateral carbody acceleration standard deviation (g)	0.13	0.11	0.09	0.08
Maximum vertical acceleration (g)	0.90	0.27	0.24	0.22
Maximum vertical suspension deflection (%)	95%	31%	31%	22%

*These tests were performed with non-instrumented wheel sets having a KR tread profile

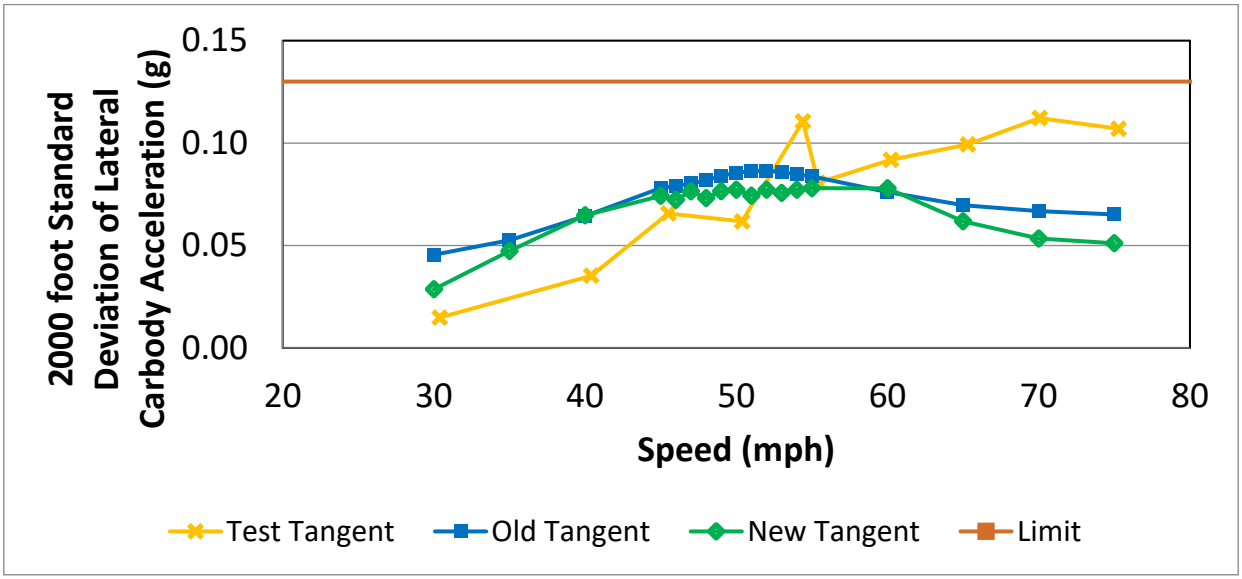


Figure 19. Simulation prediction and test results of maximum 2,000-foot standard deviation of lateral carbody acceleration in the hunting regime

7.8 Curving with Various Lubrication Conditions

Simulations of curving with various lubrication conditions were performed according to S-2043, Paragraph 4.3.11.5. Constant curving simulations were conducted in a 10-degree curve with the coefficient of friction conditions shown in Table 19. Simulations were performed using a new wheel profile on a new rail profile and with a hollow wheel profile on a ground rail profile. Figure 20 shows the worn wheel and rail profiles used for the simulations. The worn wheels were 2 mm hollow and the ground high rail profile had significant gage corner relief. The right side is the high rail in this plot. The gap between the rail profile in red and the wheel profile in blue on the gage corner of the rail represents a distinctive two-point contact condition. The lubrication and profile conditions are designed to show performance when the wheelset cannot provide normal steering forces.

Table 19. Wheel/Rail Coefficients of Friction for the Curving with Various Lubrication Conditions Regime

Friction Coefficient	High Rail Crown	High Rail Gage Face	Low Rail Crown
Case 1	0.5	0.5	0.5
Case 2	0.5	0.2	0.5
Case 3	0.5	0.2	0.2
Case 4	0.2	0.2	0.5



Figure 20. Worn wheel profiles on the ground rail profiles.
The wheelset is shifted to the high rail in the position it would be in a left-hand curve

Table 20 shows the worst-case simulation predictions for curving with various lubrication conditions. Figure 21 shows the maximum truck side L/V ratio plotted against speed to show the trend in performance. Simulation predictions with the revised model did not meet S-2043 criteria for truck side L/V ratio. This exception occurred for counterclockwise runs with Case 2 lubrication and the worn wheel profile at 12 and 24 mph. Simulations met S-2043 criteria for curving with various lubrication conditions during clockwise runs for this lubrication and profile case, and for all runs with other lubrication and profile combinations.

Table 20. Simulation predictions for curving with various lubrication conditions

Criterion	Limiting Value	Simulation Prediction Original Model	Simulation Prediction Revised Model
Roll angle (degree)	4.0	0.5	0.5
Maximum wheel L/V	0.8	0.60	0.59
95th percentile single wheel L/V (constant curving tests only)	0.6	0.57	0.56
Maximum truck side L/V	0.5	0.49	**0.52**
Minimum vertical wheel load (%)	25%	70%	69%
Lateral peak-to-peak acceleration (g)	1.3	0.20	0.23
Maximum lateral acceleration (g)	0.75	0.16	0.17
Maximum vertical acceleration (g)	0.90	0.14	0.15
Maximum vertical suspension deflection (%)	95%	35%	35%

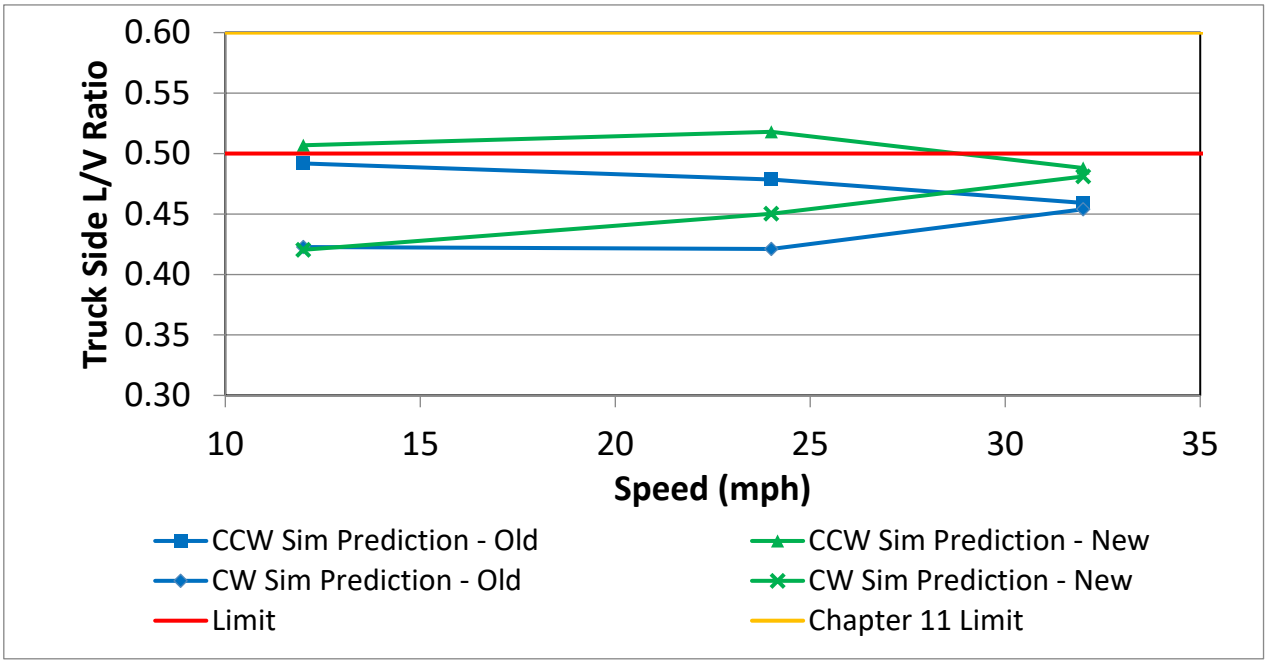


Figure 21. Simulation predictions of maximum truck side L/V ratio in the curving with various lubrication conditions regime. Case 2 lubrication with worn profiles

7.9 Turnouts and Crossovers

Simulations of the turnouts and crossovers regime were conducted according to S-2043, Paragraph 4.3.11.7. Simulations were performed through a No. 7 crossover with straight point turnouts on 13-foot track centers at speeds up to 15 mph. Simulations of the turnouts alone were not repeated with the revised model.

Table 21 shows the worst-case simulation predictions for turnouts and crossovers. Figure 22 shows the maximum truck side L/V ratio plotted against speed to show the trend in performance. Simulation predictions met S-2043 criteria for turnouts and crossovers.

Table 21.Turnout and crossover simulation predictions

Criterion	Limiting Value	Simulation Prediction Original Model	Simulation Prediction Revised Model
Roll angle (degree)	4.0	0.3	0.3
Maximum wheel L/V	0.8	0.68	0.64
Maximum truck side L/V	0.5	0.49	**0.50**
Minimum vertical wheel load (%)	25%	75%	74%
Lateral peak-to-peak acceleration (g)	1.3	0.21	0.19
Maximum lateral acceleration (g)	0.75	0.13	0.13
Maximum vertical acceleration (g)	0.90	0.17	0.16
Maximum vertical suspension deflection (%)	95%	16%	23%

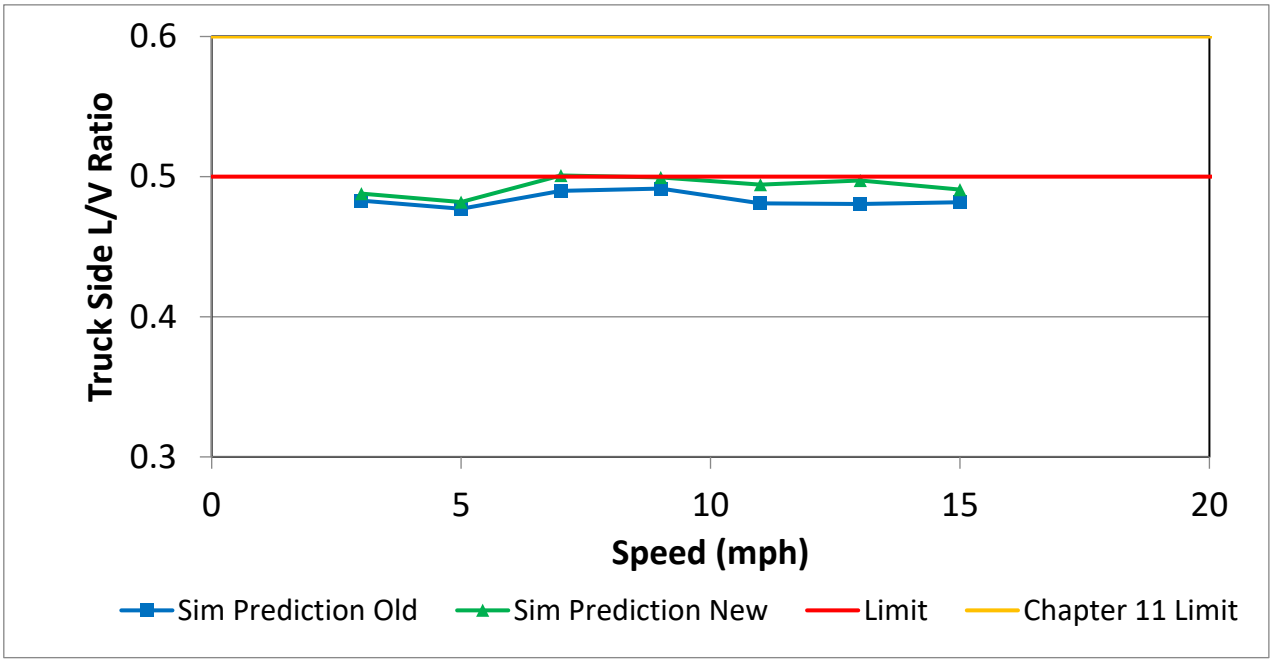


Figure 22. Simulation predictions of maximum truck side L/V ratio in the turnouts and crossovers regime

7.10 Buff and Draft Curving

Simulations of the buff and draft curving regime were conducted according to S-2043, Paragraph 4.3.13. Simulations were performed using measured track geometry of the 12-degree curve of the Wheel/Rail Mechanism Loop at TTC. Simulations were designed to simulate the car coupled to:

- A base car as described in the AAR MSRP Section C-II, Standard M-1001 Chapter 2, Paragraph 2.1.4.2.31.
- A long car having 90-foot over strikers, 66-foot truck centers, 60-inch couplers, and conventional draft gear.
- Like car (coupled to another buffer car).
- Atlas cask car – A car the buffer railcar may be coupled to in HLRM service.
- Rail Escort Vehicle (REV) – A car the buffer railcar may be coupled to in HLRM service.
- Four-axle locomotive – A vehicle the buffer railcar may be coupled to in HLRM service.
- Six-axle locomotive – A vehicle the buffer railcar may be coupled to in HLRM service.

The geometry of the coupled cars was used to calculate the longitudinal and lateral components that would be applied to the car under 250,000 pounds buff and 250,000 pounds draft. These component forces were applied to the carbody in the simulation.

Table 22 shows the worst-case simulation predictions for buff and draft curving. The highest wheel L/V ratios occurred with the buffer car coupled between two base cars and with the buffer car coupled between the REV and the Atlas cask car under draft forces. Figure 23 shows the maximum truck side L/V ratio plotted against speed to show the trend in performance for these two cases. The original simulation predictions did not meet S-2043 truck side L/V ratio criteria for buff and draft curving for cases with the car coupled between two base cars and cases with the car coupled between the Atlas car and the REV. All other S-2043 criteria were met. Simulation predictions with the revised model produced slightly lower truck side L/V ratios that met S-2043 criteria.

Table 22. Buff and draft curving simulation predictions

Criterion	Limiting Value	Simulation Prediction Original Model	Simulation Prediction Revised Model
Roll angle (degree)	4.0	0.7	0.8
Maximum wheel L/V	0.8	0.54	0.54
Maximum truck side L/V	0.5	**0.51**	**0.50**
Minimum vertical wheel load (%)	25%	54%	54%
Lateral peak-to-peak acceleration (g)	1.3	0.15	0.21
Maximum lateral acceleration (g)	0.75	0.15	0.18
Maximum vertical acceleration (g)	0.90	0.13	0.14
Maximum vertical suspension deflection (%)	95%	58%	56%

1 Association of American Railroads. 2011. *Manual of Standards of Recommended Practices*. Section C-II Design, Fabrication, and Construction of Freight Cars, Standard M-1001, Chapter 2. General Data, Paragraph 2.1.4.2.3 “Base Car.” Washington, DC.

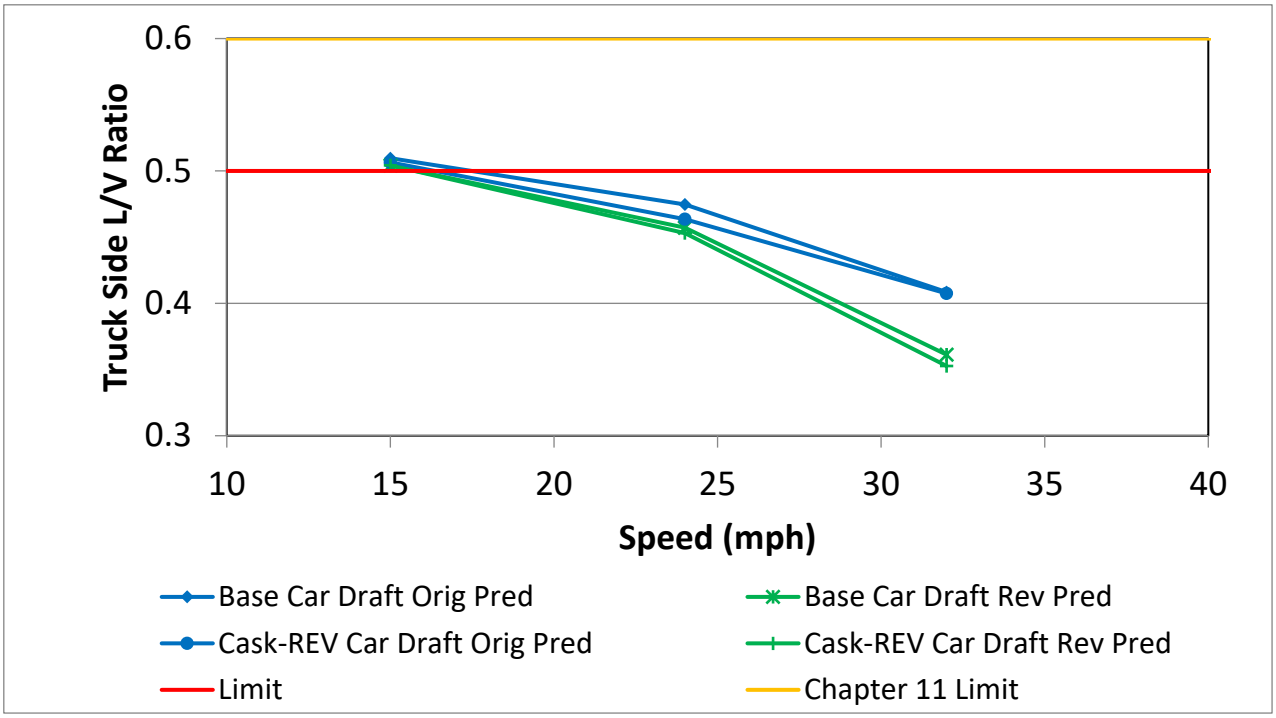


Figure 23. Simulation predictions of maximum truck side L/V ratio in the buff and draft curving regime

8.0 CONCLUSIONS

The buffer car met all S-2043 single-car structural and dynamic test requirements.

FEA simulations and structural test strain measurements both showed that stresses were less than 75 percent of the allowable stress — thus eliminating the requirement in S-2043, Paragraph 8.1 for the FEA to be refined. The largest difference between measured and predicted stress was 5.7 ksi on SGBF11 during the compressive end load test. The other three measurements in similar locations, SGBF10, SGBF37, and SGBF35 were closer to the predicted stress.

The revised model did not meet the criterion for peak-to-peak carbody lateral acceleration for the 39-foot wavelength inputs (1.38g, limit=1.3g) or the 44.5-foot wavelength inputs (1.31g, limit=1.3g) in yaw and sway. In contrast, the buffer car met test requirements for yaw and sway indicating that the model is conservative. The yaw and sway test is only performed with 39-foot wavelength inputs.

The revised modeling predictions did not meet criteria for truck side L/V ratio (0.52, limit=0.5) in the curving with various lubrication conditions regime. This exception occurred for counterclockwise runs with Case 2 lubrication and the worn wheel profile at 12 and 24 mph. The Case 2 lubrication condition is a 0.5 coefficient of friction on the top of both rails and a 0.2 coefficient of friction on the gage face to the high rail. Simulations meet S-2043 criteria for curving with various lubrication conditions during clockwise runs for this lubrication and profile case and for all runs with other lubrication and profile combinations.

Table 23 shows a summary of test results and model predictions for the buffer car.

Table 23. Summary of Simulation Predictions and Test Results

S-2043 Section	Met/Not Met		
	Preliminary Simulations	Revised Simulations	Test Result
5.2 Nonstructural Static Tests			
4.2.1/5.2.1 Truck Twist Equalization	Met	Not Simulated	Met
4.2.2/5.2.2 Carbody Twist Equalization	Met	Not Simulated	Met
4.2.3/5.2.3 Static Curve Stability	Met	Not Simulated	Met
4.2.4/5.2.4 Horizontal Curve Negotiation	Met	Not Simulated	Met
5.4 Structural Tests			
5.4.2 Squeeze (Compressive End) Load	Met	Not Required	Met
5.4.3 Coupler Vertical Loads	Met	Not Required	Met
5.4.4 Jacking	Met	Not Required	Met
5.4.5 Twist	Met	Not Required	Met
5.4.6 Impact	Met	Not Required	Met
5.5 Dynamic Tests			
4.3.11.3/5.5.7 Hunting	Met	Met	Met
4.3.9.6/5.5.8 Twist and Roll	Met	Met	Met
5.5.9 Yaw and Sway	Met	Not Met P-P Lat Accel 1.38 Limit=1.3	Met
5.5.10 Dynamic Curving	Met	Met	Met
4.3.9.7/5.5.11 Pitch and Bounce (Chapter 11)	Met	Met	Met
4.3.9.7/5.5.12 Pitch and Bounce (Special)	Met	Met	Met
4.3.10.1/5.5.13 Single Bump Test	Met	Not Simulated	Met
4.3.11.6/5.5.14 Curve Entry/Exit	Met	Not Simulated	Met
4.3.10.25.5.15 Curving with Single Rail Perturbation	Met	Met	Met
4.3.11.4/5.5.16 Standard Chapter 11 Constant Curving	Met	Not Simulated	Met
4.3.11.7/5.5.17 Special Trackwork	Met	Not Simulated	Met
4.3.11.5 Curving with Various Lubrication Conditions	Met	Not Met Truck Side L/V 0.52, Limit=0.50	Not Required
4.3.12 Ride Quality	Met	Not Simulated	Not Required
4.3.13 Buff and Draft Curving	Not Met Truck Side L/V 0.51, Limit=0.50	Met	Not Required
4.3.14 Braking Effects on Steering	Met	Not Simulated	Not Required
4.3.15 Worn Component Simulations	Met	Not Simulated	Not Required

References

1. AAR *Manual of Standards and Recommended Practices*, Car Construction Fundamentals and Details, Performance Specification for Trains Used to Carry High-Level Radioactive Material, Standard S-2043, Effective: 2003; Last Revised: 2017, Association of American Railroads, Washington, D.C.

2. Walker, Russell, M. Jones, B. Whitsitt, and R. Joy, October 30, 2020, "AAR Standard S-2043 Single-Car Certification Tests of U.S. Department of Energy Atlas Railcar Design Project Buffer Railcar" Report P-20-032, Transportation Technology Center, Inc., Pueblo, CO

3. Walker, Russell and S. Trevithick, Rev. November 20, 2017, "S-2043 Certification: Preliminary Simulations of Kasgro Buffer Railcar," Report P-17-023, Transportation Technology Center, Inc., Pueblo, CO.

TRANSPORTATION TECHNOLOGY CENTER, INC.
A wholly owned subsidiary of the Association of American Railroads

55500 DOT Road • Pueblo, CO 81001
www.aar.com

For questions or comments on this document, contact first_last@aar.com

MxV Rail

(formerly TTCI)

350 Keeler Parkway
Pueblo, Colorado USA 81001

A subsidiary of the Association of American Railroads (AAR)

www.mxvrail.com